

# New estimation of the nuclear de-excitation line emission from the supernova remnant Cassiopeia A

Bing Liu<sup>1,2,3</sup>, Rui-zhi Yang<sup>1,2,3</sup>★, Xin-yu He<sup>3,4</sup>, Felix Aharonian<sup>5,6,7</sup>

<sup>1</sup>Deep Space Exploration Laboratory/School of Physical Sciences, University of Science and Technology of China, Hefei 230026, China

<sup>2</sup>CAS Key Laboratory for Research in Galaxies and Cosmology, Department of Astronomy, School of Physical Sciences, University of Science and Technology of China, Hefei, Anhui 230026, China

<sup>3</sup>School of Astronomy and Space Science, University of Science and Technology of China, Hefei, Anhui 230026, China

<sup>4</sup>Key Laboratory of Dark Matter and Space Astronomy, Purple Mountain Observatory, Chinese Academy of Sciences, Nanjing 210023, China

<sup>5</sup>Dublin Institute for Advanced Studies, School of Cosmic Physics, 31 Fitzwilliam Place, Dublin 2, Ireland

<sup>6</sup>Max-Planck-Institut für Kernphysik, Saupfercheckweg 1, 69117 Heidelberg, Germany

<sup>7</sup>Yerevan State University, 1 Alek Manukyan St, Yerevan 0025, Armenia

Accepted XXX. Received YYY; in original form ZZZ

## ABSTRACT

MeV nuclear de-excitation lines serve as a unique tool to study low-energy cosmic rays (CRs), containing both spectral and elemental information of the interacting material. In this paper, we estimated the possible nuclear de-excitation lines from the young supernova remnant Cassiopeia A. Given different CR spectral shapes and interacting materials, we found the predicted fluxes of strong narrow line emissions from the remnant are highly model-dependent, ranging from about  $1 \times 10^{-10} \text{ cm}^{-2} \text{ s}^{-1}$  to  $1 \times 10^{-6} \text{ cm}^{-2} \text{ s}^{-1}$  for the 4.44 MeV narrow line and from about  $4 \times 10^{-11} \text{ cm}^{-2} \text{ s}^{-1}$  to  $2 \times 10^{-7} \text{ cm}^{-2} \text{ s}^{-1}$  for the 6.13 MeV narrow line, respectively. Based on the new estimation, we also discussed the detection probability of these line emissions against the MeV diffuse Galactic background under different assumptions of instrument response functions.

**Key words:** cosmic rays – gamma-rays: ISM – ISM: individual objects: Cassiopeia A – ISM: supernova remnants

## 1 INTRODUCTION

Cosmic rays (CRs) with kinematic energy below 1 GeV/nucleon, often referred to as low-energy CRs (LECRs), are most efficient at ionizing and heating gases and play an important role in star-forming and astrochemistry processes (Papadopoulos 2010; Gabici 2022). In the direct measurement of CR spectra in the solar system, the flux of LECRs is highly suppressed by the solar modulation effects. Recently, the Voyager satellite has measured the LECR spectra beyond the heliopause (Cummings et al. 2016). However, it is not straightforward that the LECR spectra measured by Voyager can be a good representative of the LECRs in the Galaxy. Due to the fast cooling and slow propagation of LECRs, their flux indirectly estimated via the ionization rate of gases shows a rather inhomogeneous distribution in the Galactic plane (e.g., Indriolo & McCall 2012).

Supernova remnants (SNRs) are thought to be the most prominent CR accelerators in our Galaxy. The  $\gamma$ -ray observations in the energy range of 0.1 – 10 GeV from AGILE and Fermi-LAT have shown strong evidence that the SNRs do accelerate CR protons to

a high energy range (Giuliani et al. 2011; Ackermann et al. 2013). Observations of the large ionization rates from molecular material near SNRs, such as IC 443, W28, and W49B, suggest that SNRs may also accelerate a large population of LECRs (Indriolo et al. 2010; Vaupré et al. 2014; Zhou et al. 2022). However, due to the kinetic energy threshold of the pion-decay process ( $\sim 280$  MeV), we know little about the injection spectrum of LECRs from SNRs. In addition to the ionization effects, the inelastic collisions between LECRs and interstellar gases could excite the heavy nuclei which can emit MeV  $\gamma$ -ray lines via de-excitation, such as the 4.44 MeV line from  $^{12}\text{C}$  and the 6.13 MeV line from  $^{16}\text{O}$  (e.g., Ramaty et al. 1979; Murphy et al. 2009). Thus, from observation of these line emissions, we may derive unique information about the injection of LECR nuclei from the accelerators such as SNRs, with the advantage of excluding the influence of CR electrons (e.g., Benhabiles-Mezhoud et al. 2013; Liu et al. 2021).

Cassiopeia A (Cas A, G111.7-02.1) is the remnant of a massive star explosion  $\sim 340$  years ago (Fesen et al. 2006; Krause et al. 2008). As one of the youngest SNRs in our Galaxy, Cas A has been thoroughly investigated from multiwavelength observations despite many open questions that remain debatable. Located about 3.4 kpc away from the solar system (Reed et al. 1995), it is one

★ E-mail: yangrz@ustc.edu.cn

of the brightest sources in the radio band and shows a significant shell structure with an angular radius of  $2.5'$  (or physical size of 2.5 pc) (Kassim et al. 1995). The synchrotron radiation extends from infrared (Tuffs et al. 1997) to X-rays of about 100 keV (Grefenstette et al. 2017). Although the origin of the X-ray radiation is still under debate, Laming (2001a,b) argued that non-thermal bremsstrahlung can also explain the observed X-ray flux. Early Fermi-LAT observations reveal a hint of the hadronic origin of the  $\gamma$ -ray emissions (Abdo et al. 2010; Yuan et al. 2013). TeV signal from Cas A was also detected (Puehlhofer 1999), and a significant cutoff at several TeV was revealed by MAGIC and VERITAS observations (Ahnen et al. 2017; Abeysekara et al. 2020). Despite the continuous debate about whether Cas A is a PeVatron or not, a pure hadronic or hybrid origin is preferred to the pure leptonic scenario when explaining the GeV–TeV  $\gamma$ -ray emission from Cas A (e.g., Zirakashvili et al. 2014; Ahnen et al. 2017; Zhang & Liu 2019; Abeysekara et al. 2020). Thus, one would expect possible MeV de-excitation line emissions arising from Cas A accelerated LECR nuclei interacting with the surrounding medium.

In this study, we investigate the potential MeV nuclear line emission from Cas A under different assumptions of the injected CR spectra which are constrained by recent observations in the GeV–TeV range. Various scenarios of the interacting medium are also considered in the calculations applying the latest estimation of the chemical abundances of the ejecta and ambient gas. Moreover, the detection capabilities of the line emissions against the continuum background are also discussed regarding the angular resolutions and energy resolutions of the next-generation MeV telescopes.

## 2 CR SPECTRA AND THE MEDIUM COMPOSITION AROUND CAS A

Before the calculation of the possible de-excitation  $\gamma$ -ray line emission from Cas A, we need to have a general idea of the spectral shape of the accelerated particles and the composition of the interacting medium. Both factors have huge impacts on the estimation results. Given the angular resolution of the next generation MeV telescopes (typically  $\gtrsim 2^\circ$  at MeV band) and the distance of Cas A, the line emission from Cas A is very likely to be observed as a point-like source (Liu et al. 2021). Thus, the spatial distributions of the accelerated LECRs, the interacting medium, as well as the resulting line emission will not be considered in this work.

### 2.1 Spectral distribution of the Cas A accelerated particles

SNRs are widely accepted as one kind of the main CR sources in our Galaxy, and they are expected to accelerate relativistic particles with spectra close to simple power laws in momentum  $p$  via the diffusive shock acceleration (e.g., Bell 1978; Blandford & Ostriker 1978). Given the "test-particle" limit, the CR production rate  $q \propto p^{-\chi}$  and the momentum index  $\chi \gtrsim 2$  in the case of strong shocks. However, when the nonlinear effects are considered, i.e., the feedback of CR energy and pressure on the shock, the accelerated particles may have spectra that show some concavity in momentum space, and the corresponding low-energy flux will be higher than that of the test-particle predictions (e.g., Amato & Blasi 2005; Caprioli et al. 2011).

The energy loss times of the injected protons with kinetic energy  $E$  of 1 MeV and 10 MeV are about  $2 \times 10^3$  yrs and  $4 \times 10^4$  yrs assuming an average medium density of  $10 \text{ cm}^{-3}$ . Given the relatively young age of Cas A, the deformation of the CR spectra

from the freshly injected spectra of Cas A could be ignored. Thus, for simplicity, we chose a piece-wise power law in proton momentum  $p(E)$  with an exponential cutoff at  $E_{\text{cut}}$  to describe the spectral distribution of CR protons. The injection flux  $F(E)$  is given by

$$F(E) = \begin{cases} N_0 \left[ \frac{p(E)}{p(E_b)} \right]^{-\alpha_1} \exp \left[ \frac{-p(E)}{p(E_{\text{cut}})} \right], & \text{if } E \geq E_b \\ N_0 \left[ \frac{p(E)}{p(E_b)} \right]^{-\alpha_2} \exp \left[ \frac{-p(E)}{p(E_{\text{cut}})} \right], & \text{if } E < E_b \end{cases} \quad (1)$$

Here, the cutoff energy  $E_{\text{cut}} = 10 \text{ TeV}$  and the broken energy  $E_b$  is set to be 0.2 GeV, below which the protons do not participate in the pion production process and lose their energy mainly via the ionization process.

### 2.2 Elemental abundances of the interacting medium

According to multiwavelength observations, the ejecta of Cas A is dominated by oxygen ( $\sim 2.55 M_\odot$ ), and the rest is comprised mainly of Ne, Si, S, Ar, and Fe, with a total mass of about 3–3.5  $M_\odot$ , meanwhile, the composition of the circumstellar medium (CSM) shows enhancement of N and He relative to the solar abundances and the mass of the shocked CSM is about 10  $M_\odot$  (e.g., Chevalier & Kirshner 1978, 1979; Docenko & Sunyaev 2010; Hwang & Laming 2012; Laming & Temim 2020). The ejecta abundances vary with position in the remnant. For example, the study of the X-ray-emitting ejecta in Cas A using the *Chandra* 1 Ms observation see sub-solar ratios (Hwang & Laming 2012), while the study of "bulk" unshocked ejecta using the IR Spitzer data get super-solar ratios (Laming & Temim 2020). To carry on our estimation, regardless of the very large uncertain remains for the exact compositions of the ejecta, we refer to the "average" number density ratios (relative to O) summarized in Table 9 from Docenko & Sunyaev (2010) for Ne, Mg, Si, S, Ar, and Fe, and adopt the solar value (relative to O) for C, N, and Ca. In addition, we change the density ratios of H and He, from 0.01 to 0.05 and 0.1 to 0.5 respectively, to check the impact of their uncertain densities in the ejecta on the flux of the line emission.

For the CSM, same as Hwang & Laming (2012), we set the abundance of He 3 times the solar value, that of N 15 times the solar value, and solar values for the rest. Meanwhile, we apply the Voyager measurement of local LECRs (see Cummings et al. 2016, Table 3) as a simplified assumption of the abundance of Cas A accelerated CRs. Above elemental compositions assumed for the calculation are summarized in Table 1.

We note that a thorough investigation into the composition of Cas A accelerated particles requires comprehensive knowledge of the acceleration and escape of the particles, as well as the diffusion and mixing of them into the surrounding medium. Such kind of research is beyond the scope of this work, which only serves as an estimate that awaits valuable information from next-generation MeV  $\gamma$ -ray detectors.

## 3 POSSIBLE DE-EXCITATION LINE EMISSION FROM CAS A

For the calculation of the  $\gamma$ -ray line emissions, except for the code TALYS which is the newest 1.96 version (Koning et al. 2008; Koning et al. 2014), we applied the same procedure as described in Section 3.1 of Liu et al. (2021), which followed the method developed by Ramaty et al. (1979); Murphy et al. (2009); Benhabiles-Mezhoud et al. (2013). Two main channels of the interactions are considered

**Table 1.** The elemental compositions assumed for calculation

	CR <sup>a</sup>	Solar <sup>b</sup>	CSM <sup>c</sup>	Ejecta <sup>d</sup>
	$n_{\text{el}}/n_{\text{H}}$	$n_{\text{el}}/n_{\text{H}}$	$n_{\text{el}}/n_{\odot}$	$n_{\text{el}}/n_{\text{O}}$
H	1	1	1	0.01-0.05 <sup>e</sup>
He	$8.140 \times 10^{-2}$	$8.414 \times 10^{-2}$	3	0.1-0.5 <sup>e</sup>
C	$1.671 \times 10^{-3}$	$2.455 \times 10^{-4}$	1	0.5 <sup>e</sup>
N	$2.444 \times 10^{-4}$	$7.244 \times 10^{-5}$	15	0.1 <sup>e</sup>
O	$1.570 \times 10^{-3}$	$5.370 \times 10^{-4}$	1	1
Ne	$1.507 \times 10^{-4}$	$1.122 \times 10^{-4}$	1	0.02
Mg	$2.264 \times 10^{-4}$	$3.467 \times 10^{-5}$	1	0.005
Si	$1.898 \times 10^{-4}$	$3.388 \times 10^{-5}$	1	0.05
S	$2.087 \times 10^{-5}$	$1.445 \times 10^{-5}$	1	0.05
Ar	$4.554 \times 10^{-6}$	$3.162 \times 10^{-6}$	1	0.005
Ca	$1.195 \times 10^{-5}$	$2.042 \times 10^{-6}$	1	0.004 <sup>e</sup>
Fe	$1.152 \times 10^{-4}$	$2.884 \times 10^{-5}$	1	0.005

<sup>a</sup> Number density ratio relative to H, adopted from the Voyager measurement of local LECR abundance (see Cummings et al. 2016, Table 3).

<sup>b</sup> Number density ratio relative to H, adopted the recommended present-day solar abundance (see Lodders 2010, Table 6).

<sup>c</sup> Number density ratio relative to the solar value, adopted for the CSM of Cas A, mainly referred to Hwang & Laming (2012).

<sup>d</sup> Number density ratio relative to O, mainly adopted from Docenko & Sunyaev (2010).

<sup>e</sup> The details for the settings of these elements are described in Sec.2.2.

here. One is the *direct* process in which the CR protons and  $\alpha$ -particles as projectiles excite heavier elements of the ambient gas and generate narrow  $\gamma$ -ray lines, and the other is the *inverse* process in which the hydrogen and helium of the ambient gas excite the heavy nuclei of LECRs and produce  $\gamma$ -ray line emission that is broadened.

Given the large difference in the elemental compositions between the ejecta and the CSM, here we consider three cases to study the possible influence of various interacting materials. One case (hereafter referred to as case 1) is that the  $\gamma$ -ray emission is generated from the shock-accelerated nuclei interacting only with the ejecta. The second one (case 2) is that the emission is produced by the accelerated nuclei colliding with the CSM. Moreover, a hybrid case (case 3) in which half of the accelerated CRs interact with the ejecta while the other half of the CRs interact with the CSM is also calculated. An estimation of the  $\gamma$ -ray lines from the same population of CRs colliding with the gas medium of solar abundance is also made for further comparison.

For each case, we tested possible proton spectra with different assumptions of  $\alpha_1$  ranging from 2.0 to 2.7 while setting  $\alpha_2 = \alpha_1$ , 3.0, and 4.0, respectively. Meanwhile, the GeV-TeV  $\gamma$ -ray spectral data from recent research of Abeyssekara et al. (2020) are used to constrain the overall flux of the accelerated particles, which provides us a maximum for  $N_0$  given a certain density and composition of the interacting medium. Here we applied the Eq.(20) in Kafexhiu et al. (2014) to calculate the nuclear enhancement factor  $\epsilon$ , then derived the effective density  $\epsilon n_p n_{\text{H}}$  for the pion-decay process, in which  $n_p$  represents the density of the accelerated protons and  $n_{\text{H}}$  is hydrogen density of the interacting medium. Examples of the pion-decay emissions derived from the above spectral parameter settings are shown in Fig.1.

Considering the uncertainty of the relative density of H and He in the ejecta, we varied their number ratios from 0.01 to 0.05 and from 0.1 to 0.5, respectively, for the calculation of case 1. We found that such changes have very little impact ( $\lesssim 3\%$ ) on the

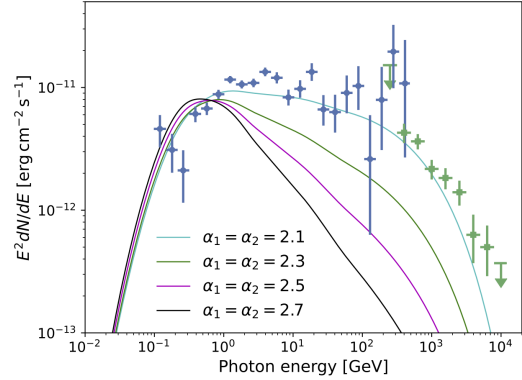


**Figure 1.** Examples of the  $\gamma$ -ray emission produced via pion-decay process from Cas A with various assumptions of  $\alpha_1$  and  $\alpha_2$ . The data points are adopted from the GeV-TeV  $\gamma$ -ray observations of Abeyssekara et al. (2020). Details are described in Sec.2.1.

overall line flux under the premise of oxygen domination. For a more realistic estimation, we also considered the Doppler effect caused by the movement of the ejecta (e.g., Milisavljevic & Fesen 2013), and adopted an  $\Delta V$  of  $\sim 6000 \text{ km s}^{-1}$  from the recent study of Picquenot et al. (2021) for all the elements. The resulting MeV nuclear de-excitation line emissions for case 1 are exemplified in Fig. 2. As shown in Fig. 2, the line fluxes increase with the spectral index and the presence of a concavity in momentum space will lead to much stronger line emissions. In addition, the same trend is also found for case 2 and case 3. However, assuming the same CR spectral shape, the line fluxes of case 2, are much lower compared to that of case 1, and the morphological difference of the MeV  $\gamma$ -ray emission is also very obvious, as illustrated by the solid lines in Fig. 3. Such contrast reflects the much more abundant heavier nuclei in the oxygen-dominated ejecta compared to those in the CSM. Taking the possible Doppler broadening into account, for case 1 and case 3, the FWHM widths ( $\Delta E$ ) of the 4.44 MeV line and the 6.13 MeV line are  $\sim 0.19 \text{ MeV}$  and  $\sim 0.22 \text{ MeV}$ , respectively. The integrated narrow-line fluxes of the 4.44 MeV and the 6.13 MeV lines of these three cases are summarized in Table 2, in which the minimum and maximum are obtained when setting  $\alpha_1 = \alpha_2 = 2.0$  and  $\alpha_1 = 2.7, \alpha_2 = 4.0$ , respectively. As shown in Table 2, the integrated line flux ranges are  $\sim (1 \times 10^{-10} - 1 \times 10^{-6}) \text{ cm}^{-2} \text{ s}^{-1}$  for the 4.44 MeV narrow line and  $\sim (4 \times 10^{-11} - 2 \times 10^{-7}) \text{ cm}^{-2} \text{ s}^{-1}$  for the 6.13 MeV narrow line, respectively.

Our estimation of the integrated 4.44 MeV line flux assuming  $\alpha_1 = \alpha_2 = 2.1$  for case 1 is  $\sim 1.4 \times 10^{-8} \text{ cm}^{-2} \text{ s}^{-1}$ , much lower compared to the estimation of Summa et al. (2011). Indeed, the target density, composition of the medium, and the LECR flux can vary dramatically with the distance to the forward shock. Using a uniform density and composition can be quite biased in estimating the MeV line emission. This is also the motivation that we consider three cases in the discussions above.

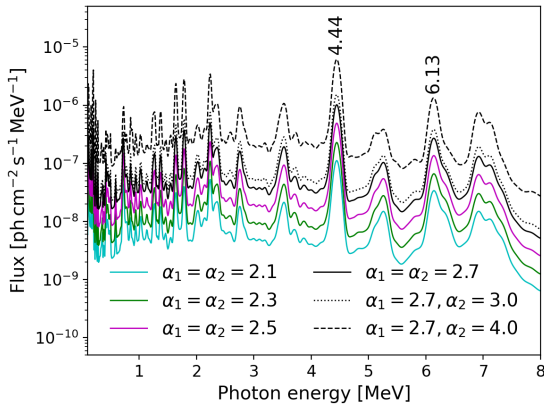
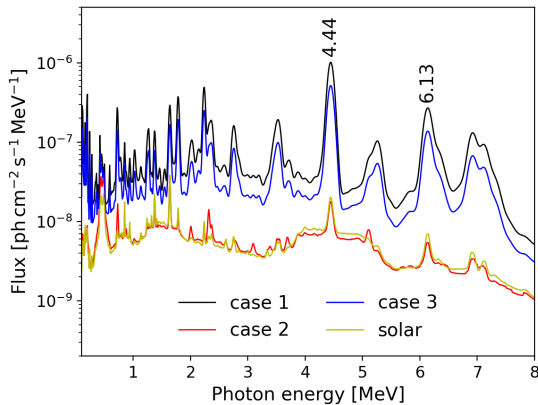
## 4 DISCUSSION AND CONCLUSION

Regardless of the uncertainties from the experiment data and the simulation data from TALYS, as shown in Sect.3, the de-excitation line fluxes resulting from the interaction between the Cas A accelerated CR nuclei and the medium are highly model-dependent: for certain cases, the predicted line fluxes vary by two orders of mag-

**Table 2.** Integrated 4.44 MeV and 6.13 MeV line fluxes of various cases <sup>a</sup>

	Medium	4.44 MeV	6.13 MeV
case 1	Ejecta	$(0.09\text{--}7.71)\times 10^{-7}$	$(0.04\text{--}2.10)\times 10^{-7}$
case 2	CSM	$(0.10\text{--}8.84)\times 10^{-9}$	$(0.04\text{--}2.66)\times 10^{-9}$
case 3	Ejecta+CSM	$(0.05\text{--}3.93)\times 10^{-7}$	$(0.02\text{--}1.06)\times 10^{-7}$

<sup>a</sup> The flux ranges (in units of  $\text{cm}^{-2} \text{s}^{-1}$ ) are obtained from different assumptions of CR spectral index ( $\alpha_1$  and  $\alpha_2$ ). Details are described in Sec.3.

**Figure 2.** Comparison of estimated MeV  $\gamma$ -ray differential spectra with different spectral settings of  $\alpha_1$  and  $\alpha_2$  for case 1 as described in Sec.3.**Figure 3.** Comparison of estimated MeV  $\gamma$ -ray differential spectra of Cas A with  $\alpha_1 = \alpha_2 = 2.7$  for different cases described in Sec.3.

nitude due to different settings of the spectral indexes, meanwhile, the narrow line fluxes could also differ by two orders of magnitude due to the variation in the elemental compositions of the interacting medium.

The continuum MeV  $\gamma$ -rays contributed from the diffuse Galactic emission and Cas A itself should be taken into account when discussing the detectability of line emission. Based on the observation of SPI aboard INTEGRAL, Siebert et al. (2022) re-analyzed the diffuse Galactic emission at 0.5 and 8.0 MeV by fitting energy-dependent spatial template GALPROP (Vladimirov et al. 2011) models within a region of  $\Delta l \times \Delta b = 95^\circ \times 95^\circ$  around the Galactic center. They found the above observed diffuse background is mainly

contributed by IC scattering of CR electrons onto the interstellar radiation field, of which the bremsstrahlung component may account for  $\sim 10\%$ . We estimate the diffuse MeV emission flux in the direction of Cas A by extrapolating this newest measurement spatially. The possible diffuse background flux in the direction of Cas A within  $1\sigma$  uncertainty is shown as the shaded area in Fig. 4 and Fig. 5, in which the angular resolutions of the telescope are assumed to be  $2^\circ$  and  $5^\circ$ , respectively. As for the continuum MeV emission from Cas A itself, which is mainly contributed from bremsstrahlung in the hadronic scenarios, the modeled fluxes are well below or at the same level of the extrapolated diffuse background (e.g., Zhang & Liu 2019; Abeyssekara et al. 2020). Thus, the potential influence from the bremsstrahlung on the detection of the line emissions would be much weaker or similar to that of the diffuse background, and for simplicity, this was not further discussed in the following discussion.

Due to the highly model-dependent calculation of the possible nuclear  $\gamma$ -ray line emission from Cas A, future observations from the next-generation MeV telescopes may help us locate the interacting region(s) and constrain the injected CR spectral shape, which can be served as a diagnosis on particle acceleration and escape in Cas A. To be specific, if the interacting material is dominated by ejecta, the strong narrow line emission such as the 4.44 MeV line and the 6.13 MeV line are more likely to be detected. Moreover, the existence of a concavity in the CR injection spectra (as exemplified by the dash-dot lines in Fig. 4), would make the detection easier for case 1 (black) and case 3 (blue), even if the flux of the background continuum is very high due to the limited angular resolution. And a better angular resolution can increase the possibility of detection for case 2 (red). In general, with the possible diffuse background emission added, the detection of the MeV line emission will be more likely from instruments with better angular resolutions ( $2.0^\circ$ ) for the point-like source SNR Cas A. In addition, we checked the influence on the detectability regarding the energy resolutions ( $\Delta E/E$ , FWHM) of the telescopes. The results are shown in Fig. 5, assuming a  $\Delta E/E$  of 2% (solid lines) or 10% (dotted lines), respectively. We found that the energy resolution is crucial for the detection of such line features. However, as calculated in the section above, we found that the narrow de-excitation lines have intrinsic Doppler broadening of about 2% that is caused by the recoil of the excited nuclei, and additional broadening of about 2% due to the movements of the ejecta-dominated medium. Thus the energy resolution better than this value can hardly improve the detection sensitivity.

In conclusion, we estimated the possible MeV line emission from LECRs interaction with the ambient gas in the SNR Cas A under simplified conditions. We found that if the accelerated CRs mainly interact with the ejecta, the line signal from Cas A will be more prominent due to the higher ratio of heavy nuclei therein. And the potential softening of LECR spectra caused by CR feedback to the shock would further enhance the MeV line emissions. We also found that the diffuse MeV  $\gamma$ -ray emissions in the Galactic plane may be the main background in the detection of such line features. Both angular resolution and energy resolution play a significant role in detecting these MeV lines from Cas A. Based on our model-dependent predication, the integrated narrow line fluxes are  $\sim 1 \times 10^{-10} \text{ cm}^{-2} \text{ s}^{-1}$  to  $1 \times 10^{-6} \text{ cm}^{-2} \text{ s}^{-1}$  at 4.44 MeV and from  $\sim 4 \times 10^{-11} \text{ cm}^{-2} \text{ s}^{-1}$  to  $2 \times 10^{-7} \text{ cm}^{-2} \text{ s}^{-1}$  at 6.13 MeV, respectively. Thus, the next generation MeV instruments with a line flux sensitivity of about  $10^{-6} \text{ cm}^{-2} \text{ s}^{-1}$ , such as e-ASTROGAM, AMEGO, and COSI (de Angelis et al. 2018; McEnery et al. 2019; Tomsick & COSI Collaboration 2022) may have chances of detecting these unique spectral features in Cas A, but detectors with

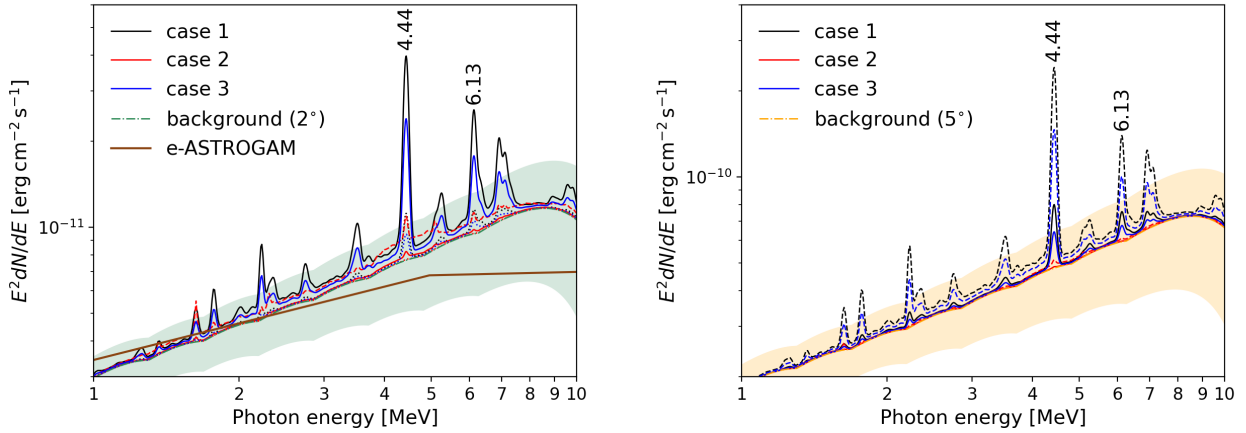


**Figure 4.** The overall MeV  $\gamma$ -ray emission from Cas A region with extrapolated diffuse background added for various cases and spectral shapes, in which  $\alpha_1 = \alpha_2 = 2.7$  is denoted by the solid lines,  $\alpha_1 = \alpha_2 = 2.1$  is denoted by the dotted lines, and  $\alpha_1 = 2.7, \alpha_2 = 4.0$  is denoted by the dashed lines. The dash-dotted line and shaded area represent possible diffuse background emission with  $1\sigma$  uncertainty around Cas A, assuming the angular resolutions of the telescope are  $2^\circ$  (green) or  $5^\circ$  (orange), respectively. The sensitivity of e-ASTROGAM calculated at  $3\sigma$  for an effective exposure of 1 year and for a source at high Galactic latitude is shown by the brown line (de Angelis et al. 2018). See Sect. 4 for the details.

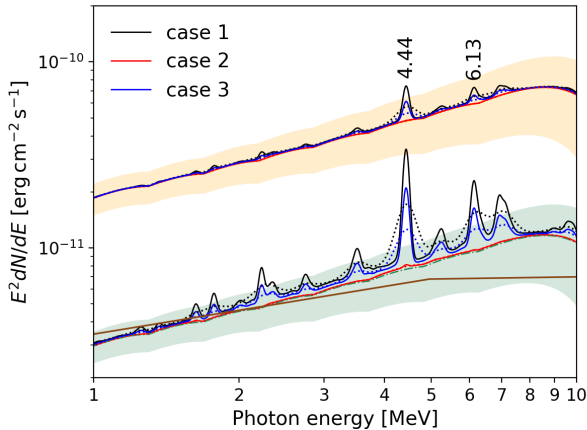


**Figure 5.** The overall MeV  $\gamma$ -ray emission from Cas A region with extrapolated diffuse background added when considering different instrument energy resolutions ( $\Delta E/E$ ) for  $\alpha_1 = \alpha_2 = 2.7$ . The assumed energy resolutions ( $\Delta E/E$ ) are 2% for solid lines and 10% for dotted lines, respectively. The dash-dotted lines, the shaded areas, and the brown line are the same as Fig. 4.

sensitivities exceeding the capability of projects mentioned above would be more promising for the research of such kind of individual CR sources. The recently proposed large-scale Space Projects like MeGaT (Zhang et al. 2023, private communication) and MeV-GRO (Peng et al. 2023, private communication) give optimism that the probes of low-energy particles from Cas A could be realized through the detection of prompt nuclear de-excitation line emission.

## 5 ACKNOWLEDGEMENTS

Bing Liu acknowledges the support from the NSFC under grant 12103049. Rui-zhi Yang is supported by the NSFC under grants

12041305, and the national youth thousand talents program in China.

## 6 DATA AVAILABILITY

To calculate emissivities of the de-excitation  $\gamma$ -ray line lines, we used the code TALYS (version 1.96, Koning et al. (2008)), which could be downloaded from [https://tendl.web.psi.ch/tendl\\_2019/talys.html](https://tendl.web.psi.ch/tendl_2019/talys.html). For a better match with the experiment data, we modified the deformation files of  $^{14}\text{N}$ ,  $^{20}\text{Ne}$ , and  $^{28}\text{Si}$  using the results of Benhabiles-Mezhoud et al. (2011). We also used the production cross sections of the specific lines listed in the compilation of Murphy et al. (2009).

## REFERENCES

- Abdo A. A., et al., 2010, *The Astrophysical Journal*, 710, L92  
 Abeyssekera A. U., et al., 2020, *ApJ*, 894, 51  
 Ackermann M., et al., 2013, *Science*, 339, 807  
 Ahnen M. L., et al., 2017, *MNRAS*, 472, 2956  
 Amato E., Blasi P., 2005, *MNRAS*, 364, L76  
 Bell A. R., 1978, *MNRAS*, 182, 147  
 Benhabiles-Mezhoud H., et al., 2011, *Phys. Rev. C*, 83, 024603  
 Benhabiles-Mezhoud H., Kiener J., Tatischeff V., Strong A. W., 2013, *ApJ*, 763, 98  
 Blandford R. D., Ostriker J. P., 1978, *ApJ*, 221, L29  
 Caprioli D., Blasi P., Amato E., 2011, *Astroparticle Physics*, 34, 447  
 Chevalier R. A., Kirshner R. P., 1978, *ApJ*, 219, 931  
 Chevalier R. A., Kirshner R. P., 1979, *ApJ*, 233, 154  
 Cummings A. C., et al., 2016, *The Astrophysical Journal*, 831, 18  
 Docenko D., Sunyaev R. A., 2010, *A&A*, 509, A59  
 Fesen R. A., et al., 2006, *ApJ*, 645, 283  
 Gabici S., 2022, *A&ARv*, 30, 4  
 Giuliani A., et al., 2011, *ApJ*, 742, L30  
 Grefenstette B. W., et al., 2017, *ApJ*, 834, 19  
 Hwang U., Laming J. M., 2012, *ApJ*, 746, 130  
 Indriolo N., McCall B. J., 2012, *ApJ*, 745, 91  
 Indriolo N., Blake G. A., Goto M., Usuda T., Oka T., Geballe T. R., Fields B. D., McCall B. J., 2010, *ApJ*, 724, 1357

- Kafexhiu E., Aharonian F., Taylor A. M., Vila G. S., 2014, *Phys. Rev. D*, **90**, 123014
- Kassim N. E., Perley R. A., Dwarakanath K. S., Erickson W. C., 1995, *ApJ*, **455**, L59
- Koning A. J., Hilaire S., Duijvestijn M. C., 2008, in Bersillon O., Gunsing F., Bauge E., Jacqmin R., Leray S., eds, Proceedings of the International Conference on Nuclear Data for Science and Technology, April 22-27, 2007, Nice, France. EDP Sciences. pp 211–214, doi:10.1051/ndata:07767
- Koning A., Rochman D., van der Marck S., 2014, *Nuclear Data Sheets*, **118**, 187
- Krause O., Birkmann S. M., Usuda T., Hattori T., Goto M., Rieke G. H., Misselt K. A., 2008, *Science*, **320**, 1195
- Laming J. M., 2001a, *ApJ*, **546**, 1149
- Laming J. M., 2001b, *ApJ*, **563**, 828
- Laming J. M., Temim T., 2020, *ApJ*, **904**, 115
- Liu B., Yang R.-z., Aharonian F., 2021, *A&A*, **646**, A149
- Lodders K., 2010, *Astrophysics and Space Science Proceedings*, **16**, 379
- McEnery J., et al., 2019, in Bulletin of the American Astronomical Society. p. 245 (arXiv:1907.07558)
- Milisavljevic D., Fesen R. A., 2013, *ApJ*, **772**, 134
- Murphy R. J., Kozlovsky B., Kiener J., Share G. H., 2009, *ApJS*, **183**, 142
- Papadopoulos P. P., 2010, *ApJ*, **720**, 226
- Picquetot A., Acero F., Holland-Ashford T., Lopez L. A., Bobin J., 2021, *A&A*, **646**, A82
- Puehlhofer G., 1999, in 26th International Cosmic Ray Conference (ICRC26), Volume 3. p. 492
- Ramaty R., Kozlovsky B., Lingenfelter R. E., 1979, *ApJS*, **40**, 487
- Reed J. E., Hester J. J., Fabian A. C., Winkler P. F., 1995, *ApJ*, **440**, 706
- Siebert T., Bertheaud J., Calore F., Serpico P. D., Weinberger C., 2022, *A&A*, **660**, A130
- Summa A., Elsässer D., Mannheim K., 2011, *A&A*, **533**, A13
- Tomsick J., COSI Collaboration 2022, in 37th International Cosmic Ray Conference. p. 652 (arXiv:2109.10403), doi:10.22323/1.395.0652
- Tuffs R. J., Drury L. O., Fischera J., Heinrichsen I., Rasmussen I., Russel S., Völk H. J., 1997, in Heras A. M., Leech K., Trams N. R., Perry M., eds, ESA Special Publication Vol. 419, The first ISO workshop on Analytical Spectroscopy. p. 177
- Vaupré S., Hily-Blant P., Ceccarelli C., Dubus G., Gabici S., Montmerle T., 2014, *A&A*, **568**, A50
- Vladimirov A. E., et al., 2011, *Computer Physics Communications*, **182**, 1156
- Yuan Y., Funk S., Jóhannesson G., Lande J., Tibaldo L., Uchiyama Y., 2013, *ApJ*, **779**, 117
- Zhang X., Liu S., 2019, *ApJ*, **874**, 98
- Zhou P., et al., 2022, *ApJ*, **931**, 144
- Zirakashvili V. N., Aharonian F. A., Yang R., Oña-Wilhelmi E., Tuffs R. J., 2014, *ApJ*, **785**, 130
- de Angelis A., et al., 2018, *Journal of High Energy Astrophysics*, **19**, 1

This paper has been typeset from a  $\text{\TeX}/\text{\LaTeX}$  file prepared by the author.